

Dynamic computer-generated nonlinear-optical hologramsHaigang Liu,^{1,2} Jun Li,³ Xiangling Fang,^{1,2} Xiaohui Zhao,^{1,2} Yuanlin Zheng,^{1,2,*} and Xianfeng Chen^{1,2,†}¹*State Key Laboratory of Advanced Optical Communication Systems and Networks, Department of Physics and Astronomy, Shanghai Jiao Tong University, Shanghai 200240, China*²*Key Laboratory for Laser Plasma (Ministry of Education), Collaborative Innovation Center of IFSA, Shanghai Jiao Tong University, Shanghai 200240, China*³*Science and Technology College, Jiangxi Normal University, Jiangxi 330027, China*

(Received 16 October 2016; revised manuscript received 29 June 2017; published 1 August 2017)

We propose and experimentally demonstrate dynamic nonlinear optical holograms by introducing the concept of computer-generated holograms for second-harmonic generation of a structured fundamental wave with a specially designed wave front. The generation of Laguerre-Gaussian second-harmonic beams is investigated in our experiment. Such a method, which only dynamically controls the wave front of the fundamental wave by a spatial light modulator, does not need domain inversion in nonlinear crystals and hence is a more flexible way to achieve the off-axis nonlinear second-harmonic beams. It can also be adopted in other schemes and has potential applications in nonlinear frequency conversion, optical signal processing, and real-time hologram, etc.

DOI: [10.1103/PhysRevA.96.023801](https://doi.org/10.1103/PhysRevA.96.023801)

The holography technique [1,2], which records the amplitude and phase of a wave from an illuminated object, has been developed for decades since it was proposed. In the linear-optical field, it has been widely used in optical tweezing [3,4], microscopy [5], quantum information [6], and optical communication [7,8]. Moreover, it has also blossomed and yielded fruit in many other fields as a powerful tool of wave shaping, such as acoustics [9,10], microwaves [11], electron beams [12,13], and surface-plasmon-polariton waves [14]. In some fields, with the development of modulators, the holography technique has been pushed to the dynamical manipulation of the amplitude and/or phase of the wave, leading to the emergence of computer-generated holograms (CGHs). Nevertheless, in other fields, the development of the dynamic nature of the holography technique seems to have come to a standstill.

In recent years, shaping a generated wave front of a light wave via nonlinear processes has attracted more and more interest, with a variety of methods having been proposed. One of the methods was to design the spatial structure of nonlinear photonic crystals (NPCs) to shape the phase of the generated second-harmonic (SH) beam [15–27]. The holography concept has also been introduced to the nonlinear field by shaping the nonlinear light wave in one-dimensional (1D) or 2D manners [16–18]. In addition, nonlinear volume holography has also been proposed and realized in recent years [19,20]. Another method to shape the nonlinear light wave was assisted by a functional facet [28]. However, in these works, attention is paid to the design of the NPCs or the functional facet, which lacks flexibility owing to complex fabrication and the unchangeable spatial structure of the media. The disadvantage can be mitigated by introducing a technique capable of manipulating the light wave front in a dynamical way to the nonlinear holography.

In previous research, a few works focused on controlling the nonlinear light wave by varying the input fundamental beam [29–31]. We also proposed that a specially designed structured fundamental wave (FW) could be used to generate a nonlinear Raman-Nath SH dynamically [32]. The method allows for the dynamical control of the structure of the FW by utilizing a spatial light modulator (SLM). Moreover, the modulated FW can propagate along any direction of a bulk nonlinear medium. This is important for highly efficient second-harmonic generation (SHG) by utilizing larger components of the $\chi^{(2)}$ tensor. Hence, this method can naturally be expected as a potential way to realize dynamic computer-generated nonlinear optical holograms.

In this paper the concept of dynamic computer-generated nonlinear optical holograms is proposed and experimentally demonstrated. When a FW beam with an intentionally modulated wave front passes through a bulk nonlinear medium, a wave front with the desired amplitude and phase can be obtained in the first order of the SH. In our experiment, amplitude-modulated Laguerre-Gaussian (LG) (including LG₁₀ and LG₂₀) SH beams are generated in the first order. In addition to the amplitude-modulated case, a meaningful and interesting case of only a phase-modulated vortex beam is analyzed with the topological charge $l_{SH} = ql_1$ for the q th ($m + n = q$)-order SH. Another case of LG₁₁ with both the modulated amplitude and phase is also generated in the experiment.

The phase of the FW is modulated in the form $\vec{E}_1 = \text{sgn}\{\cos[2\pi f(\vec{r}, \varphi) + \phi(x, y)] - \cos[\pi b(x, y)]\} \exp[i(\vec{k}_1 \cdot \vec{z} - \omega t)]$, which supposes that the FW propagates along the z direction. Here $\vec{r} = x\vec{x} + y\vec{y}$, $\varphi = \tan^{-1}(y/x)$ is the azimuthal angle, $f(r, \varphi) = |\vec{r}|\cos(\varphi)/\Lambda$ is the frequency of the carrier function, $b(x, y)$ and $\phi(x, y)$ are the functions of the amplitude and phase of the encoded information, respectively, and \vec{k}_1 is the wave vector of the FW. For the long-period modulation of the FW, its diffraction can be negligible in a sufficiently short medium. In the experiments, the modulated period of the FW and the length of the crystal are 78 μm and 0.5 mm, respectively, which meets the condition of nondiffraction according to the analysis in [32]. Under the nondiffraction

*ylzheng@sjtu.edu.cn

†xfchen@sjtu.edu.cn

approximation, the expansion of a Fourier series of such a FW can be written as

$$\vec{E}_1 = \sum_{m=-\infty}^{+\infty} \left\{ \frac{\sin[m\pi b(x,y)]}{m\pi} \exp\{im[2\pi f(\vec{r},\varphi) + \phi(x,y)]\} \right\} \times \exp[i(\vec{k}_1 \cdot \vec{z} - \omega t)]. \quad (1)$$

We define the expression of the SH wave as $\vec{E}_2 = A_2 \exp[-i(k_{2t} \cdot \vec{r} + k_{2z}z - 2\omega t)]$, where A_2 , k_{2t} , and k_{2z} are the amplitude and transverse and longitudinal wave vectors of the SH, respectively. According to the coupled wave equation, the evolution of the SH wave is directly given by [17,32]

$$\frac{dA_2}{dz} = \kappa \chi^{(2)} A(x,y) \sum_q^{m+n=q} \{ \exp[iq\phi(x,y)] \} \exp[i2k_1z - ik_{2z}z] \times \exp[iq2\pi f(\vec{r},\varphi) - i\vec{k}_{2t} \cdot \vec{r}], \quad (2)$$

where

$$A(x,y) = \sum_q^{m+n=q} \left\{ \frac{\sin[m\pi b(x,y)]}{m\pi} \times \frac{\sin[n\pi b(x,y)]}{n\pi} \right\}$$

and $\varphi(x,y) = q\phi(x,y)$ are the respective amplitude and phase of the generated SH, which is the Fourier transform (FT) of the desired wave front in the q th diffraction order. Hence, the phase information of the FW can be directly achieved for a given SH beam. However, it is completely different from the linear or nonlinear CGH in Ref. [18], in which $A(x,y) = \sin[m\pi b(x,y)]$ and $b(x,y)$ is in the range $[0,0.5]$. The amplitude modulation in our method is the sum of infinite terms. For a given $A(x,y)$, the solution of $b(x,y)$ is not unique. For a given SH beam, the amplitude information of the FW can be restored by numerical calculation. The relation between $A(x,y)$ and $b(x,y)$ is shown in Fig. 1(a). In our experiments, the desired SH modes were obtained at the first diffraction order. The first nine terms are chosen in the calculation and $b(x,y)$ is controlled in the range of $[0, 0.273]$ for the purpose of keeping $A(x,y)$ and $b(x,y)$ injective.

To demonstrate the concept of dynamic computer-generated nonlinear optical holograms, we chose to design the structure of the FW aimed to generate three modes in the LG families, i.e., LG_{10} , LG_{20} , and LG_{11} , in the first diffraction order. The transverse spatial distribution of LG modes propagating in the z direction is

$$E_{l,p}(r,\varphi,z) = \frac{C_{lp}^{LG}}{\omega(z)} \left(\frac{r\sqrt{2}}{\omega(z)} \right)^{|l|} \exp\left(-\frac{r^2}{\omega^2(z)}\right) L_p^{|l|} \left(\frac{2r^2}{\omega^2(z)} \right) \times \exp(-il\varphi), \quad (3)$$

where C_{lp}^{LG} are the normalized constants of LG beams, $\omega(z) = \omega_0 \sqrt{1 + (z\lambda/\pi\omega_0^2)^2}$ and ω_0 are the local beam radius and beam waist, respectively, $L_p^{|l|}(u)$ is a generalized Laguerre polynomial, and l is the topological charge of the LG mode. Since the FT of a LG mode is the same, the modulation of the FW can be calculated according to Eq. (3).

The experimental setup is shown in Fig. 1(b). The laser source was a Nd:YAG nanosecond laser at a wavelength

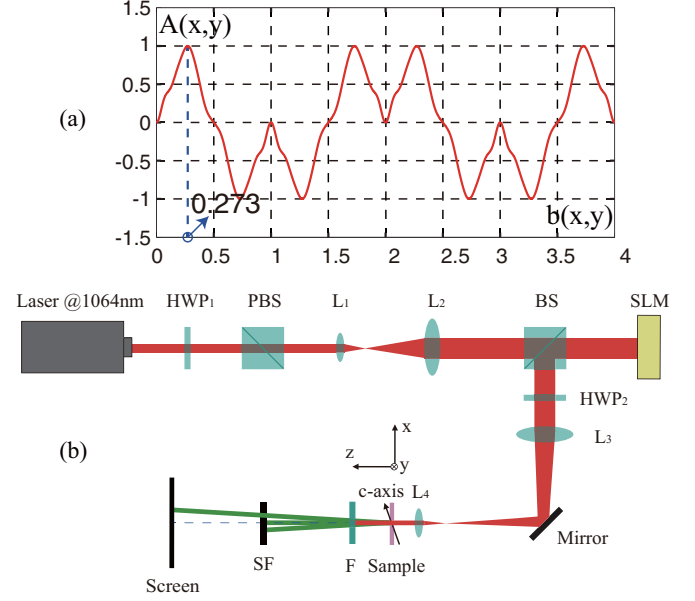


FIG. 1. (a) Relation between $A(x,y)$ and $b(x,y)$. (b) Schematic of the experimental setup to realize dynamic computer-generated nonlinear optical holograms. The following denotations are used: HWP, half-wave plate; PBS, polarization BS; $L_{1,\dots,4}$, lens; $f_{1,\dots,4} = 50, 100, 200,$ and 50 mm, respectively; BS, beam splitter; SLM, spatial light modulator; Sample: 5 mol% MgO:LiNbO₃; F, filter; and SF, spatial filter.

of 1064 nm. A half-wave plate HWP₁ and a polarization beam splitter were used to control the polarization and intensity of the FW. Lenses L₁ and L₂ were used to expand and collimate the FW incident onto the SLM. The SLM had a resolution of 512×512 pixels, each with a rectangular area of $19.5 \times 19.5 \mu\text{m}^2$. The updating speed of the nonlinear holograms was determined by the refresh rate (75 Hz) of the SLM. The half-wave plate HWP₂ was used to control the polarization of the FW. The FW was imaged by a 4- f system (consisting of L₃ and L₄) to imprint the modulated wave-front pattern onto a $\chi^{(2)}$ crystal. The beam waist was reduced to 2 mm. After the crystal, the short-pass filter (F) was used to filter out the FW. The +1 order of the SH was obtained after a spatial filter. Finally, the generated SH beam was projected on a screen in the far field and recorded by a camera. For simplicity and without loss of generality, the sample of a 5 mol % MgO:LiNbO₃ thin bulk crystal was used (0.5 mm thick). The FW was kept as o polarized and the process was type I (oo-e) phase matched. The FW propagated along the birefringent phase matching (BPM) direction (at room temperature, the angle is 75° with respect to the c axis of the crystal, according to the Sellmeier equation in [33]).

According to the analysis, the designed phase structures of the FW shown in Figs. 2(a)–2(c) correspond to LG_{10} , LG_{20} , and LG_{11} , respectively. The frequency of modulation in the x direction and the period of all the FWs were chosen to be $78 \mu\text{m}$. Hence, $f(\vec{r},\varphi)$ is $0.0128 \mu\text{m}^{-1}$ and the first diffraction order can be obtained at an external angle of $\lambda_{\text{SH}} f(\vec{r},\varphi) \sim 6.28$ mrad, where λ_{SH} is the SH wavelength. The desired LG modes in theory can be obtained at the first diffraction order,

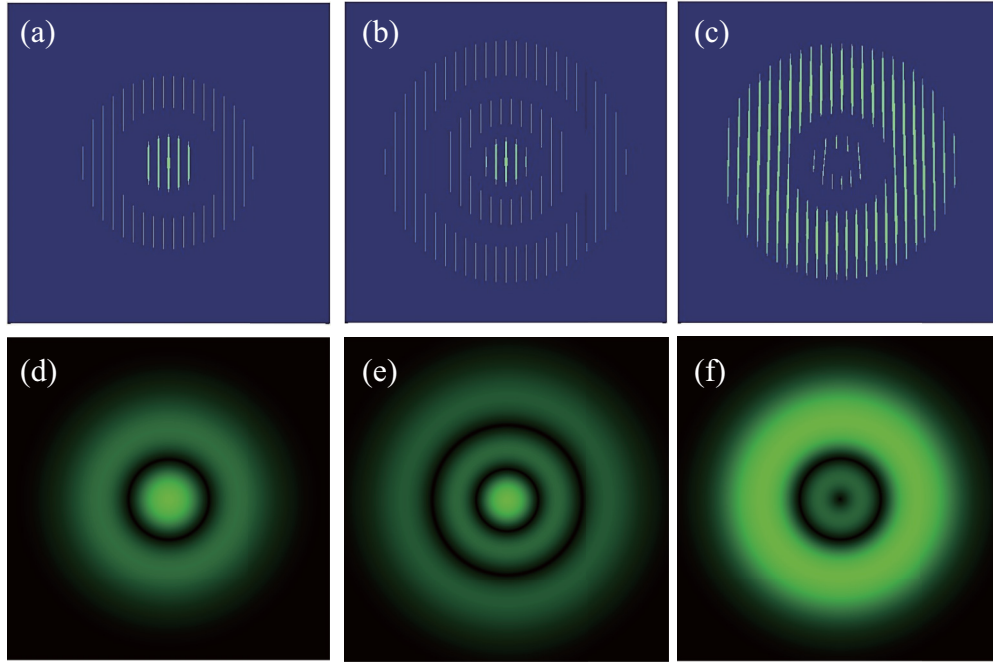


FIG. 2. Phase structures of the FW with $0-\pi$ phase modulation corresponding to (a) LG_{10} , (b) LG_{20} , and (c) LG_{11} and profiles of calculated SH beams corresponding to (d) LG_{10} , (e) LG_{20} , and (f) LG_{11} .

as shown in Figs. 2(d)–2(f) corresponding to LG_{10} , LG_{20} , and LG_{11} , respectively.

Figures 3(a) and 3(b) show the experimental results of the amplitude-modulation cases corresponding to LG_{10} and LG_{20} beams. According to Eq. (2), the phase of SH is $\varphi(x, y) = q\phi(x, y) = (m + n)\phi(x, y)$. When the FW is modulated in the form of a fork-shaped structure with phase $\phi(x, y) = ml_1\varphi$, the topological charge of the SH is $l_{SH} = ql_1$ for the q th ($m + n = q$) order. It means that the orbital angular momentum is added through the nonlinear process, so a fork-shaped phase-modulated fundamental beam can be converted to a series of SH vortex beam that is the same as that in the fork-shaped NPCs, as in [17]. Interestingly, although it is a SH process, it still possesses a linear grating property, in which $l_{SH} = ql_1$ for the q th-order SH. In fact, the orbital angular momentum of the SH [$l_{SH} = ql_1 = (m + n)l_1$] comes from different orders of FWs.

In addition to the phase-modulation case, another meaningful and interesting case of the SH vortex beam, namely, the LG_{11} SH beam, carrying a topological charge of $l = 1$, is studied, in which the amplitude and also the phase modulation are studied at the same time. The profile of the calculated LG_{11} beams is illustrated in Fig. 2(f) and the experiment result is shown in Fig. 3(c).

The cross section of the simulated (solid red curve) and measured (dashed blue curve) intensities was also compared, shown in Figs. 3(d)–3(f), corresponding to LG_{10} , LG_{20} , and LG_{11} , respectively. In fact, there are two factors that can cause the distortions with respect to the theoretical simulation. First, free-space holograms are usually optically thin, thereby providing a well-defined plane of amplitude and phase patterns for the illuminating free-space beam. The reason for the SH distortions may be that the thickness (0.5 mm in our experiment) of the nonlinear crystal in the propagation direction

cannot be neglected. Second, the inaccuracy of the 4- f system in the experiment, in which the phase structure of the FW cannot be accurately imprinted onto the nonlinear crystal, may also cause the distortion of the generated SH beams.

In our method, the FW source used is a Nd:YAG laser producing 4-ns pulses at a 20-Hz repetition rate at a wavelength of 1064 nm. The energy of one pulse of the laser is 1 mJ. In principle, the total conversion efficiency, calculated for average power, of such BPM in the propagating direction is $18.5\% W^{-1}$ and the measured one is approximately $12.5\% W^{-1}$. The predicted conversion efficiency for peak power is $1.48 \times 10^{-6}\% W^{-1}$ and the measured one is $1 \times 10^{-6}\% W^{-1}$. The percentages of the desired SH beams are 9.28%, 9.81%, and 19.15%, corresponding to LG_{10} , LG_{20} , and LG_{11} , respectively. The lower conversion efficiency in the experiment mainly comes from the Fresnel losses at the nonlinear crystal facets. In the case of the SH shaping method along the transverse direction of a binary modulated NPC [17,18], the conversion efficiency for average power and peak power are about $10^{-7}\% W^{-1}$ and $10^{-12}\% W^{-1}$, respectively. With the absence of key parameter information about the laser in Refs. [17,18], it is difficult to compare the conversion efficiency for the same conditions. However, we believe that the conversion efficiency of our method is much higher under the same conditions, such as the same length of the crystal and the same parameters of the laser, because, under the same conditions, the different conversion efficiency mainly arises from the scheme of the phase matching manner between our method and Refs. [17,18], which are BPM and nonlinear Raman-Nath phase matching, respectively.

The method of dynamic computer-generated nonlinear optical holograms introduced in this paper features many advantages over the off-axis nonlinear SH shaping in NPCs. Limited by the domain inversion technique [34], only 1D SH

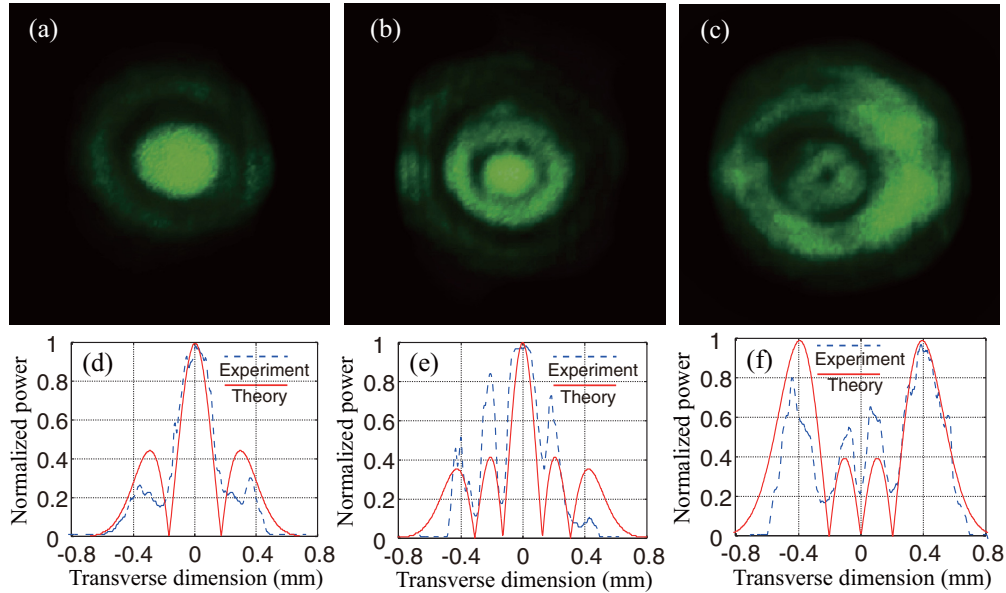


FIG. 3. Generated SH beams in experiment corresponding to (a) LG_{10} , (b) LG_{20} , and (c) LG_{11} and cross section of the simulated (solid red curve) and measured (dashed blue curve) intensities corresponding to (d) LG_{10} , (e) LG_{20} , and (f) LG_{11} .

beam shaping can be realized [15,19,21,26] using quasiphase matching schemes. The method to realize 2D SH shaping proposed by Shapira and co-workers is that of the fundamental Gaussian beam propagating along the z axis of NPCs [16–18,20]. However, the quite low conversion efficiency is caused by the phase mismatch. Our method not only allows for shaping the amplitude and phase of the SH at the same time in 2D cases, but also possesses a higher conversion efficiency than the methods in [16–18,20] as the FW can be propagating along any direction of the nonlinear crystal (in this paper, the FW propagates along the BPM direction). However, it should be mentioned that, for the purpose of keeping the nondiffraction assumption valid, long transverse modulated periods of the FW and the sufficient short interaction length need to be satisfied at the same time. These two factors limit the conversion efficiency and spatial frequencies of the generated SH pattern in our method.

Dynamic computer-generated nonlinear optical holograms can be used to dynamically generate arbitrary shapes of beams and are not limited to only LG beams, such as the Airy beam [35]. They also can be employed for other desired wave fronts and provide full control of the amplitude and phase of the converted beam dynamically.

In conclusion, we proposed and experimentally demonstrated dynamic nonlinear optical holograms by introducing the concept of CGHs for SHG of a structured FW with a specially designed wave front. In our experiment, amplitude-modulated LG (including LG_{11} and LG_{20}) SH beams were generated. In addition to the amplitude-modulated case, the case of only a phase-modulated vortex beam was analyzed with the topological charge $l_{SH} = ql_1$ for the q th ($m + n = q$)-order SH. Another case of the LG_{11} SH beam with both the modulated amplitude and phase was also generated in the experiment. Such a method does not require domain inversion for nonlinear crystals, only dynamic control of the phase of the FW by a SLM, and hence is a more flexible way to achieve the off-axis nonlinear SH beams. It also can be adopted in other schemes and has potential application in nonlinear frequency conversion, optical signal processing, real-time hologram, etc.

This work was supported in part by the National Natural Science Foundation of China under Grants No. 61125503, No. 61235009, and No. 11421064 and the Foundation for Development of Science and Technology of Shanghai under Grant No. 13JC1408300.

-
- [1] D. Gabor, *Nature (London)* **161**, 777 (1948).
 [2] J. J. Burch, *Proc. IEEE* **55**, 599 (1967).
 [3] L. Huang, H. Guo, J. Li, L. Ling, B. Feng, and Z. Li, *Opt. Lett.* **37**, 1694 (2012).
 [4] H. He, M. E. J. Friese, N. R. Heckenberg, and H. Rubinsztein-Dunlop, *Phys. Rev. Lett.* **75**, 826 (1995).
 [5] T. Vettenburg, H. I. C. Dalgarno, J. Nylk, C. Coll-Llado, D. E. K. Ferrier, T. Cizmar, F. J. Gunn-Moore, and K. Dholakia, *Nat. Meth.* **11**, 541 (2014).
 [6] X. L. Wang, X. D. Cai, Z. E. Su, M. C. Chen, D. Wu, L. Li, N. L. Liu, C. Y. Lu, and J. W. Pan, *Nature (London)* **518**, 516 (2015).
 [7] J. Wang, J. Y. Yang, I. M. Fazal, N. Ahmed, Y. Yan, H. Huang, Y. X. Ren, Y. Yue, S. Dolinar, and M. Tur, *Nat. Photon.* **6**, 488 (2012).
 [8] G. Milione, T. A. Nguyen, J. Leach, D. A. Nolan, and R. R. Alfano, *Opt. Lett.* **40**, 4887 (2015).
 [9] K. Melde, A. G. Mark, T. Qiu, and P. Fischer, *Nature (London)* **537**, 518 (2016).

- [10] D. Baresch, J. L. Thomas, and R. Marchiano, *Phys. Rev. Lett.* **116**, 024301 (2016).
- [11] Y. Aoki, *Appl. Opt.* **6**, 1943 (1967).
- [12] N. Voloch-Bloch, Y. Lereah, Y. Lilach, A. Gover, and A. Arie, *Nature (London)* **494**, 331 (2013).
- [13] G. Plascencia-Villa, A. Ponce, J. F. Collingwood, M. J. Arellano-Jimenez, X. W. Zhu, J. T. Rogers, I. Betancourt, M. Jose-Yacaman, and G. Perry, *Sci. Rep.* **6**, 24873 (2016).
- [14] I. Epstein, Y. Tsur, and A. Arie, *Laser Photon. Rev.* **10**, 360 (2016).
- [15] T. Ellenbogen, N. V. Bloch, A. G. Padowicz, and A. Arie, *Nat. Photon.* **3**, 395 (2009).
- [16] A. Shapira, I. Juwiler, and A. Arie, *Opt. Lett.* **36**, 3015 (2011).
- [17] N. V. Bloch, K. Shemer, A. Shapira, R. Shiloh, I. Juwiler, and A. Arie, *Phys. Rev. Lett.* **108**, 233902 (2012).
- [18] A. Shapira, R. Shiloh, I. Juwiler, and A. Arie, *Opt. Lett.* **37**, 2136 (2012).
- [19] X. H. Hong, B. Yang, C. Zhang, Y. Q. Qin, and Y. Y. Zhu, *Phys. Rev. Lett.* **113**, 163902 (2014).
- [20] B. Yang, X. H. Hong, R. E. Lu, Y. Y. Yue, C. Zhang, Y. Q. Qin, and Y. Y. Zhu, *Opt. Lett.* **41**, 2927 (2016).
- [21] S. Trajtenberg-Mills, I. Juwiler, and A. Arie, *Laser Photon. Rev.* **9**, L40 (2015).
- [22] A. Shapira, I. Juwiler, and A. Arie, *Laser Photon. Rev.* **7**, L25 (2013).
- [23] S. Lightman, R. Gvishi, G. Hurvitz, and A. Arie, *Opt. Lett.* **40**, 4460 (2015).
- [24] A. Shapira, L. Naor, and A. Arie, *Sci. Bull.* **60**, 1403 (2015).
- [25] K. Shemer, N. Voloch-Bloch, A. Shapira, A. Libster, I. Juwiler, and A. Arie, *Opt. Lett.* **38**, 5470 (2013).
- [26] Y. Q. Qin, C. Zhang, Y. Y. Zhu, X. P. Hu, and G. Zhao, *Phys. Rev. Lett.* **100**, 063902 (2008).
- [27] T. Ellenbogen, I. Dolev, and A. Arie, *Opt. Lett.* **33**, 1207 (2008).
- [28] A. Shapira, A. Libster, Y. Lilach, and A. Arie, *Opt. Commun.* **300**, 244 (2013).
- [29] I. Dolev, I. Kaminer, A. Shapira, M. Segev, and A. Arie, *Phys. Rev. Lett.* **108**, 113903 (2012).
- [30] A. Libster-Hershko, S. Trajtenberg-Mills, and A. Arie, *Opt. Lett.* **40**, 1944 (2015).
- [31] I. Dolev and A. Arie, *Appl. Phys. Lett.* **97**, 171102 (2010).
- [32] H. G. Liu, J. Li, X. H. Zhao, Y. L. Zheng, and X. F. Chen, *Opt. Express* **24**, 15666 (2016).
- [33] O. Gayer, Z. Sacks, E. Galun, and A. Arie, *Appl. Phys. B* **91**, 343 (2008).
- [34] M. Yamada, N. Nada, M. Saitoh, and K. Watanabe, *Appl. Phys. Lett.* **62**, 435 (1993).
- [35] G. A. Siviloglou, J. Broky, A. Dogariu, and D. N. Christodoulides, *Phys. Rev. Lett.* **99**, 213901 (2007).